

Quantum superposition principle and gravitational collapse: Scattering times for spherical shells

M. Ambrus and P. Hájíček
Institute for Theoretical Physics
University of Bern
Sidlerstrasse 5, CH-3012 Bern, Switzerland

July 2005

Abstract

A quantum theory of spherically symmetric thin shells of null dust and their gravitational field is studied. In Nucl. Phys. **603** (2001) 515, it has been shown how superpositions of quantum states with different geometries can lead to a solution of the singularity problem and black hole information paradox: the shells bounce and re-expand and the evolution is unitary. The corresponding scattering times will be defined in the present paper. To this aim, a spherical mirror of radius R_m is introduced. The classical formula for scattering times of the shell reflected from the mirror is extended to quantum theory. The scattering times and their spreads are calculated. They have a regular limit for $R_m \rightarrow 0$ and they reveal a resonance at $E_m = c^4 R_m / 2G$. Except for the resonance, they are roughly of the order of the time the light needs to cross the flat space distance between the observer and the mirror. Some ideas are discussed of how the construction of the quantum theory could be changed so that the scattering times become considerably longer.

1 Introduction

The most important and difficult problems of the relativistic theory of gravitational collapse are the singularities (see, e.g., Ref. [1]) and the black-hole information paradox (Ref. [2]). In fact, there are some ideas around of how both the singularities and information losses in gravitational collapse could be avoided. An example is a pioneer work by Sacharov Ref. [3] in 60's assuming 1) that the equation of state for very dense matter is $p = -\rho < 0$ so that its stress-energy tensor is equivalent to a "cosmological" term, and 2) that the collapsed stuff will be concentrated in a small, roughly stationary, very massive but everywhere regular piece of matter with this equation of state. The space-time geometry is mostly assumed to be classical and to obey classical Einstein's equations everywhere: there seem to be no need for quantum gravity. The singularity theorems of Ref. [1] are not applicable because of the large negative pressure. For more detail and further developments see Ref. [4].

Another proposal, which does not require exotic states of matter but exploits the superposition principle of quantum theory instead, is described in Refs. [5], [6] and [7]. Let us quickly summarize what was shown and what remained unclear there. In this way, we introduce and motivate what will be done in the present paper.

The collapsing matter was represented by a spherically symmetric self-gravitating thin shell of null dust. There were no other sources of gravity and the space-time had a regular center. This was considered as a toy model of black-hole creation. From the state of the shell at a space-like 3-surface that intersects the regular center and the shell, the gravitational field can be completely determined by the constraints everywhere along the 3-surface. This was used to reduce the total action to variables that described just the state of the shell (Ref. [5]).

In the quantum theory (Refs. [6] and [7]), a self-adjoint extension of the shell Hamiltonian (depending only on the shell state variables) was chosen such that shell wave packets were formed by linear combinations of in- and outgoing states and vanished at the center. In this sense, the singularity was removed.

In principle, the quantum geometry around the shell ought to be determined by the state of the shell. The problem was that the naive straightforward calculation depended of the foliation along which the metric had to be determined, and the resulting geometry itself was, unlike in

the classical theory, *strongly* dependent on it. This was interpreted in a more general way as a failure of gauge-dependent methods in quantum gravity, which lead in turn to search for some manifestly gauge-independent methods.

Still, the nature of the quantum horizon resulting in each quantum evolution of the shell could be investigated in rough terms. It turned out that it was a linear combination of states with black- and white-hole Schwarzschild horizons. This was related to the fact that an in-going shell creates a black-hole horizon, while an outgoing one creates a white-hole horizon outside of it. Thus, the intriguing result that the shells with a sufficiently high energy could cross their Schwarzschild radius in both directions could be naturally explained. This kind of quantum horizon was called *gray horizon* in Ref. [6]. It is a superposition of black- and white-hole Schwarzschild horizons because the state of the shell is a superposition of in- and outgoing motions. Now, the in- and outgoing states are related by the time reversal, as are the white- and black-hole horizons. Thus, the time reversal seems to play some role here.

This role has to do with time reversal properties of Schwarzschild geometry, which are rather subtle. If the Schwarzschild radial coordinate R is larger than Schwarzschild radius $2M$, M being the mass parameter of the Schwarzschild solution, the geometry is *locally* time-reversal invariant: for any chosen point with $R > 2M$, there is a time-reversal map that is an isometry of the space-time and does not move the point. This is not true for most points with $R \leq 2M$. It follows, e.g., that a contracting spherically symmetric source of mass M can create the same geometry outside as the same source that expands, as long as the geometry is observed outside of $2M$. The same is true for stationary axisymmetric black-hole space-times such as Kerr's, only the time reversal is to be accompanied by an additional reversal of the azimuthal coordinate.

This qualitative argument implies that quantum geometry, whatever it might be, will differ strongly from the classical one if:

1. its (spherically symmetric) source is a superposition of in- and outgoing states,
2. the source gets under its Schwarzschild radius and
3. we measure the geometry under the Schwarzschild radius of the source.

On the other hand, there seems to be no reason why the quantum geometry outside the Schwarzschild radius had to differ much from the classical one if the first two conditions hold.

Thus, our quantum superposition idea need not contradict existence and observed properties of black-hole like objects, because these properties are in any case theoretically calculated from the classical geometry outside their horizons.

This is, however, only a speculation; one ought to calculate the quantum geometry of the bouncing shell to prove the statement. Such calculations are very difficult. Problems begin already at the observation that we do not even know how this quantum geometry is *defined*: it seems that no gauge-invariant definition of it is known. The effect of different gauge choices is large in quantum gravity. Its full extent does not seem to be adequately and sufficiently realized, although it is easy to assess. The gauge fixing in general relativity can be understood as point to point identification of manifolds with non-isometric geometries. As an example, consider the average metric of, say, two different space-times with the same topology. This notion is not well-defined (even in the classical physics), unless the two manifolds are identified point by point. The resulting value of the average depends on the identification so that, for some, it need not even be a Lorentzian metric (see also Ref. [8]).

The aim of the present work is more modest: We choose a particular measurable property of the geometry and try to calculate it. It must be gauge invariant because it is measurable but it need not contain information enough so that all measurable properties of the geometry are determined by it. Which quantity we choose? In Refs. [6] and [7], the quantum shell was shown to contract from an asymptotically flat region, bounce and expand again into the same asymptotically flat region. Hence, it must be possible for one and the same observer in this region to meet the shell first in its contracting and later in its expanding phase. He can measure the time between the two events; it is the so-called *scattering time* of the quantum shell. That is the quantity we are going to calculate.

Although the scattering time contains only a small amount of information about the quantum geometry, it is important. For example, if the scattering time is too short, the existence of the gray horizon will also be short, and nothing much can happen in its neighborhood to be observed as “the black hole properties”. If, however, the shell will come out only after many thousands of years, or if its scattering time is even larger than the age of the Universe, then the black hole object created by it would last long enough to act in its neighborhood as a black hole and to be observed. To calculate this simple quantity has turned out to be still surprisingly difficult.

In calculations based on a gauge fixing, a foliation of all space-times with in-going and outgoing shells is to be prescribed. Depending on this choice, the scattering time can take any real value! This is not the only difficulty. The *time delay* (see Refs. [9] and [10]) often used in quantum scattering theory to define the duration of a scattering process is infinite for long-ranged potential like the Coulomb or the gravitational one. While there exists a regularization of the time evolution dependent on the fixed central charge for the Coulomb potential (Ref. [11]) that renders the time delay finite (Ref. [12]), it does not work in the gravitational case because here the role of the 'central charge' is played by the energy of the shell which is not fixed but depends on the state. Since a state-dependent regularization does not make much sense, one has to abandon the hope to define the time delay in an analogous way as it was possible in Coulomb scattering.

The problem is even worse: for example, the *sojourn time* (Ref. [9]), which is finite for finite regions also in the case of long-range potentials, cannot be properly defined. The definition of the sojourn time is based on a time average, where the time integrated over is the Minkowski time in flat space-time. In the curved shell space-time it is not clear which 'time' should be chosen and an appropriate time coordinate could depend on the shell's energy, turning it into an operator in the quantum theory. Problems then arise with a sensible definition of the sojourn time because of non-commuting operators. All these difficulties can be thought of as a scattering-theory version of the so-called *problem of time* in quantum gravity (cf. Refs. [13], [14]). That's why we make a more modest approach by defining the scattering time already on the classical level and turn it into an operator in a suitable quantum theory.

Any measurable classical geometrical property can be expressed in terms of Dirac observables and "quantized" by choosing some factor ordering of the corresponding operators. However, the scattering time is not such a property because no classical shell bounces and re-expands but just disappears in the black hole it creates.

The method that will be adopted in the present work (after quite a number of different approaches have been attempted unsuccessfully) is as follows. First, we shall modify the model by introducing a spherical mirror of radius R_m . Then even a classical shell will be reflected by the mirror and there will be a gauge-invariant classical formula for the scattering time. However, a classical shell will be reflected to the asymptotic region from which it has come only if its energy

E is smaller than the *critical energy*

$$E_m = \frac{R_m c^4}{2G} .$$

$E_m c^{-2}$ is the mass whose Schwarzschild radius coincides with the radius of the mirror. A shell with $E < E_m$ will not cross its own Schwarzschild radius anywhere on its way to the mirror. Its classical scattering time will diverge if its energy approaches E_m .

Second, it will turn out that the average scattering time in the quantum theory does *not* diverge if the expected energy of the shell approaches E_m , but has only a finite peak, as if there was a resonance. One can then extend the quantum theory in an obvious way to cover energies larger than E_m . Third, we take the limit $R_m \rightarrow 0$ in such an extended theory and assume that the resulting theory gives the valid description of the quantum collapse without the mirror.

The plan of the paper is as follows. In Sec. 2, all solutions with the reflected shell are found. A complete set of Dirac observables is chosen and symmetries in the space of solutions are listed. Then the classical formula for the scattering time is derived. Sec. 3 summarizes relevant notions and equations of the Hamiltonian formalism for null shells from Louko, Whiting and Friedman paper [15] (LWF). In Sec. 4, the two LWF actions, one for in- and the other for the outgoing shells are unified and the action is modified to include the mirror and shell reflections. The mirror is considered as a formal boundary represented by some boundary conditions. This allows some freedom of how the shell is reflected especially in the quantum theory. Boundary conditions for the gravitational field and the shell at the mirror of the classical version of the theory are chosen such that the desired solutions result. Sec. 5 uses the method of Refs. [5] and [16] to reduce the action to the Dirac observables. In this way, the Poisson algebra of the observables is determined. The observables are the energy E of the shell and its canonical conjugate v , which is the asymptotic advanced time of the in-going shell.

This algebra forms a starting point for the construction of the quantum mechanics in Sec. 6. We postulate a natural cut-off E_o on energies that may be used in the scattering states; it is the energy that would create a horizon at the radius R_o of the observer. In such a way, the energy is not only positive but also bound from above. This makes it possible to find self-adjoint extensions of v . The spectrum of v is then discrete but as dense as indistinguishable from a continuous one. The scattering times and the times at which the observer meets the

shell are turned to operators after the classical formulae are extended for all scattering energies in Sec. 7. The expected values and the spreads of these operators are calculated in Sec. 7.1 for eigenstates of v . They are all finite though the classical formula has a singularity and they are independent of (the eigenvalue of) v . Sec. 7.2 studies the energy dependence of the scattering time and its spread using simple box wave packets. Two kinds of phenomena are found. First, the scattering times have a narrow peak at the critical energy E_m (where the classical formula has a singularity). This looks like a “resonance”. Second, if the energy increases beyond about $0.1 E_o$, the scattering time reaches another maximum and then begins to decrease eventually falling under zero near E_o . This is due to the changes of geometry near the observer created by the huge energy of the shell so that the scattering theory method ceases to be applicable. Sec. 8 discusses our results and methods in some broader contexts.

This paper is based on Ref. [17]

2 The model

We consider a self-gravitating, spherically symmetric and infinitesimally thin shell such as in Ref. [5]. Unlike Ref. [5], however, we introduce a spherical ideal mirror of radius R_m so that the shell and the mirror are co-centric. The shell scatters at the mirror as depicted in Fig. 1.

If such a shell of finite momentum is reflected at the mirror, the finite change of its momentum must result within an infinitesimal time interval. This requires the mirror to bear infinite force, an idealization similar to the whole notion of a thin shell, and it must be understood only as a limiting case of a regular system.

We shall view the mirror just as a boundary conditions at $R = R_m$ and consider only the part of the space-time that lies outside of the mirror. The conditions will be such that no energy and momentum can cross the boundary, and that the mass of the mirror is zero. It will be specified more precisely later. Logically, we define the solutions first, and only then infer the corresponding boundary conditions from it.

In the present section, we construct and discuss the space of solutions for the system that we have introduced in the previous paragraph. The space of solutions for a single shell without the mirror is already well-known (cf. e.g. Ref. [5]). Also the case of multiple shells has been discussed

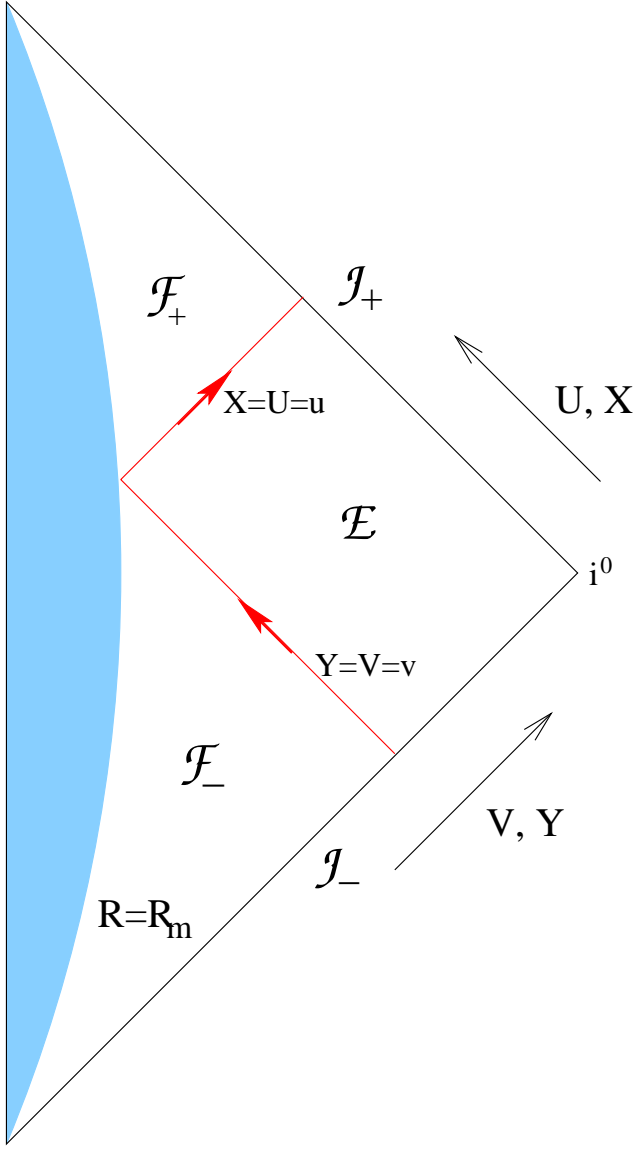


Figure 1: (Color online) Penrose-like diagram of the space-time $\bar{\mathcal{M}}$. The shaded region lies inside the mirror with the radius $R = R_m$. The in-going shell trajectory defined by $Y = V = v$ starts at past light-like infinity \mathcal{I}_- , becomes an outgoing shell trajectory $X = U = u$ at the mirror and ends up at future light-like infinity \mathcal{I}_+ . The region outside the shell is denoted by \mathcal{E} , that inside the outgoing (in-going) shell by \mathcal{F}_+ (\mathcal{F}_-). The arrows show the directions in which the double-null coordinates U and V (or X and Y) increase.

in the literature, Ref. [16]. Any solution with a reflected shell can be constructed by cutting and pasting together one solution with an in-going and one with an outgoing shell. These can be taken over from Ref. [5].

In Ref. [5], the outgoing-shell space-time is described in the double-null (DN) coordinates U and V . The metric has everywhere the form

$$ds^2 = -A_+ dU dV + R_+^2 d\Omega^2 , \quad (1)$$

where Ω^2 is the line element of a unite sphere. Outside the shell, $-\infty < U < u$,

$$A_+ = \frac{1}{\kappa(f_+) \exp(\kappa(f_+))} \frac{V - u}{4M_+} \exp\left(\frac{V - U}{4M_+}\right) , \quad (2)$$

$$R_+ = 2M_+ \kappa(f_+) , \quad (3)$$

$$f_+ = \left(\frac{V - u}{4M_+} - 1\right) \exp\left(\frac{V - U}{4M_+}\right) , \quad (4)$$

where $\kappa(x)$ is the function inverse to $\kappa^{-1}(x) = (x - 1)e^x$. Metric (1) describes Schwarzschild geometry with the mass parameter M_+ related to the outgoing-shell energy E_+ by $M_+ = Gc^{-4}E_+$. Inside the shell, $u < U < V$,

$$A_+ = 1 , \quad R_+ = \frac{V - U}{2} ; \quad (5)$$

it is Minkowski space-time. Metric (1) is continuous across the shell, $U = u$. The parameters M_+ and u have been chosen in Ref. [5] as coordinates in the space of outgoing-shell solutions.

The in-going-shell space-time, given in the DN coordinates X and Y , has the metric

$$ds^2 = -A_- dX dY + R_-^2 d\Omega^2 . \quad (6)$$

Outside the shell, $v < Y < \infty$,

$$A_- = \frac{1}{\kappa(f_-) \exp[\kappa(f_-)]} \frac{v - X}{4M_-} \exp\left(\frac{Y - X}{4M_-}\right) , \quad (7)$$

$$R_- = 2M_- \kappa(f_-) , \quad (8)$$

$$f_- = \left(\frac{v - X}{4M_-} - 1\right) \exp\left(\frac{Y - X}{4M_-}\right) , \quad (9)$$

M_- being the Schwarzschild mass parameter related to the in-going-shell energy E_- . Inside the shell $X < Y < v$,

$$A_- = 1 , \quad R_- = \frac{Y - X}{2} .$$

This is again flat space-time. The parameters M_- and v play the role of coordinates in the corresponding space of solutions.

An important property is that the solution determined by the parameters M_+ and u is isometric to that with M_- and v if $M_+ = M_-$. The isometry is described by the relations

$$U - u = v - Y \ , \quad V - u = v - X \tag{10}$$

and will be called *time reversal*.

So much about the description of the solutions in Ref. [5]. Let us now cut the outgoing-shell space-time along the curve $R = R_m$ inside the shell. The coordinate V of the intersection of this cut with the shell, $U = u$, is

$$V_0 = u + 2R_m \ . \tag{11}$$

Our cut continues outside the shell along $V = V_0$. Finally, we throw away everything inside the cut (see Fig. 2).

For the construction, the assumption is crucial that R_+ increases with decreasing U along the part of the cut that lies outside the shell, reaching eventually $R_+ = \infty$. This can only be true if R_m is larger than the Schwarzschild radius of the shell,

$$R_m > 2M_+ \ , \tag{12}$$

or

$$E_+ < E_m \ , \tag{13}$$

the critical energy (defined in the Introduction).

Similarly, we cut the in-going-shell space-time at $R = R_m$ inside the shell until the cut reaches the shell at

$$X_0 = v - 2R_m \ , \tag{14}$$

and then proceed with the cut along $X = X_0$ outside the shell and throw everything away that lies inside the cut (cf. Fig. 2). Let us further choose the parameters M_- and v as follows:

$$M_- = M_+ = M \ , \tag{15}$$

$$v = V_0 \ . \tag{16}$$

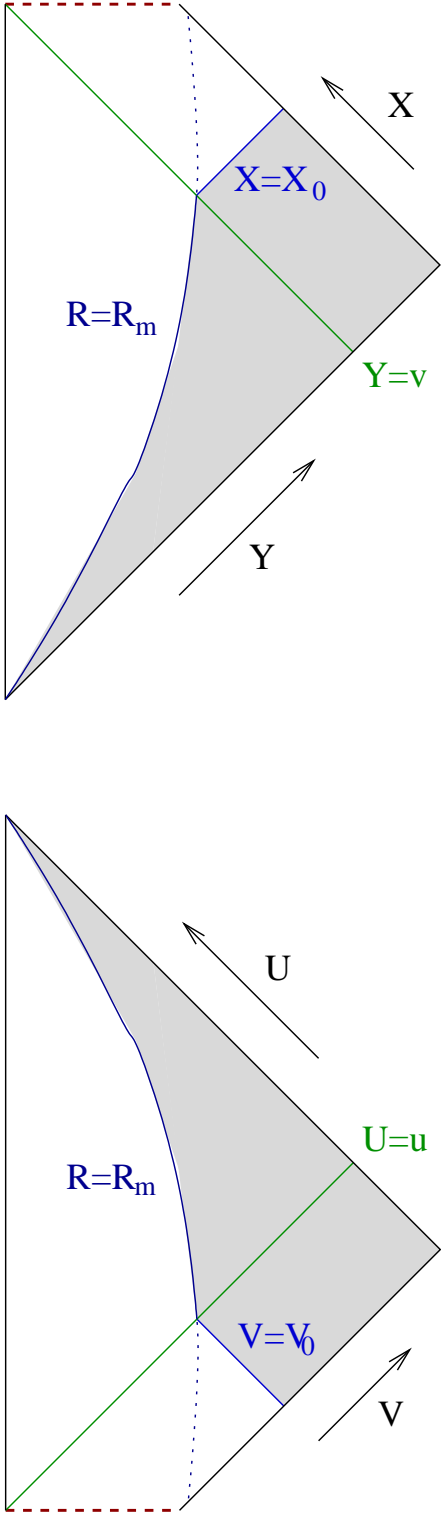


Figure 2: (Color online) The diagram on the right hand side displays the Penrose diagram of the outgoing Ref. [5] shell space-time. The shell trajectory is given by $U = u$. The shaded region is cut out and glued with the corresponding shaded region taken from the in-going space-time on the left hand side. Here, the shell trajectory is ¹⁰ given by $Y = v$. The rectangles outside of the shell are isometric.

This implies first that the outgoing null surface $X = X_0$ is diverging, R_- increasing with Y along it. Second, Eqs. (14), (16) and (11) imply

$$v = u + 2R_m \quad (17)$$

and

$$X_0 = u . \quad (18)$$

Also, the geometries of the two cut-out space-times are isometric in the patches outside the shells, that is, respectively, in $U \in (-\infty, u)$, $V \in (v, \infty)$ and $X \in (-\infty, u)$, $Y \in (v, \infty)$ and can be pasted together there by the map

$$X = v - 4M\kappa \left[\left(\frac{v-u}{4M} - 1 \right) \exp \left(\frac{v-U}{4M} \right) \right], \quad (19)$$

$$Y = u + 4M \ln \left[\frac{\kappa^{-1} \left(\frac{V-u}{4M} \right)}{\frac{v-u}{4M} - 1} \right], \quad (20)$$

resulting in the region \mathcal{E} of Fig. 1. One easily verifies that the map is an isometry and that the corresponding boundaries cover each other.

In this way, we obtain solutions in which the outgoing shell crosses the in-going one at $R = R_m$. All such solutions are described by just two parameters, M and u (or M and v , u and v being related by Eq. (17)). This defines the space of solutions of our system. Each solution is given in two coordinate patches. This will not lead to any problems later, and the fact that the coordinates of the patches coincide with the coordinates chosen in Ref. [5] will enable us to use directly many results of Ref. [5] without need for extra calculations.

In the space of solutions, we find the following symmetries.

The time shift. This is the map

$$U \mapsto U - \tau, \quad V \mapsto V - \tau, \quad X \mapsto X - \tau, \quad Y \mapsto Y - \tau, \quad (21)$$

for any real τ . The solution obtained in this way from the solution with parameters u , v , M and R_m corresponds to the change of the parameters

$$u \mapsto u + \tau, \quad v \mapsto v + \tau, \quad M \mapsto M, \quad R_m \mapsto R_m . \quad (22)$$

The dilatation. The map is defined by point shift

$$U \mapsto U/\xi, \quad V \mapsto V/\xi, \quad X \mapsto X/\xi, \quad Y \mapsto Y/\xi,$$

and metric deformation

$$g_{\mu\nu} \mapsto \xi^2 g_{\mu\nu} .$$

We obtain the solution with changed parameters

$$u \mapsto \xi u , \quad v \mapsto \xi v , \quad M \mapsto \xi M , \quad R_m \mapsto \xi R_m .$$

The most interesting question for the present paper is how long it takes till a shell returns to an observer at a fixed radius R_o : the so-called *scattering time* $s(R_o)$. The segment of the observer trajectory that is bounded by the two intersections of the shell with it lies inside each of the two patches. Let us calculate it in the coordinates U and V .

The trajectory must satisfy the equation $R_+(U, V) = R_o$; Eqs. (3) and (4) give

$$U = V - 2R_o + 4M \ln \left(\frac{V - u - 4M}{2R_o - 4M} \right) .$$

We also obtain from Eqs. (2) and (3)

$$f_+ = \kappa^{-1} \left(\frac{R_o}{2M} \right)$$

and

$$A_+ = \left(1 - \frac{2M}{R_o} \right) \frac{V - u}{V - u - 4M} .$$

The boundaries of the segment contain the crossing of the in-going shell at $V = v$ and that of the outgoing one at $U = u$, where $V = u + 2R_o = v - 2R_m + 2R_o$, according to Eq. (17). Then,

$$s(R_o) = \int_v^{v+2R_o-2R_m} dV \sqrt{A_+ \frac{dU}{dV}} ,$$

and we obtain easily

$$s(R_o) = \sqrt{1 - \frac{2M}{R_o}} \left[2(R_o - R_m) + 4M \ln \left(\frac{R_o - 2M}{R_m - 2M} \right) \right] . \quad (23)$$

Here, the first factor transforms Schwarzschild time into the proper time of the observer. The first term in the brackets is the flat-space-time scattering time (the velocity of light is set to 1) and the second term is another correction to it. Observe that this correction diverges if the energy of the shell approaches the critical energy E_m .

Another gauge-invariant quantity is the proper time measured by the observer when the shell is passing him, $s_+(R_o)$ for the outgoing and $s_-(R_o)$ for the in-going shell. We have, of course

$$s(R_o) = s_+(R_o) - s_-(R_o) . \quad (24)$$

The time $s_-(R_o)$ coincides with the flat-space-time inertial-system time T of this event. Inside the in-going shell, this time is related to X and Y by

$$T = \frac{X + Y}{2} ;$$

the shell runs along the curve $Y = v$ and the radius satisfies

$$R = \frac{-X + Y}{2} ,$$

hence

$$s_-(R_o) = v - R_o . \tag{25}$$

The other passing time, $s_+(R_o)$, can then be obtained by Eq. (24).

3 Canonical Action

We are going to describe a canonical formalism for the dynamics of the reflected shells. We start from LWF action [15] and modify it so that it describes both in- and outgoing shells; we also replace the fall-off conditions at the internal infinity or the boundary conditions at the regular center by the boundary conditions appropriate at the mirror.

Let us first summarize the relevant equations of the LWF paper. The space-time geometry is given by the ADM metric

$$ds^2 = -N^2 dt^2 + \Lambda^2 (d\rho + N^\rho dt)^2 + R^2 d\Omega^2, \tag{26}$$

where N, N^ρ, Λ, R are functions of t and ρ ; N, Λ and R are positive. $\Lambda(\rho)$ and $R(\rho)$ are canonical coordinates of the gravitational field while $P_\Lambda(\rho)$ and $P_R(\rho)$ are their conjugate momenta. The shell history is denoted by $\rho = r(t)$ and p is the momentum conjugate to ρ . A quantity Q evaluated at the shell will be denoted by $Q(r)$. Derivatives with respect to ρ are abbreviated by a prime, Q' , those with respect to t by an over-dot, \dot{Q} .

Including the null shell, the Hamiltonian bulk action reads

$$S_\eta = \int dt \left[p\dot{r} + \int_{\mathbb{R}} d\rho \left(P_\Lambda \dot{\Lambda} + P_R \dot{R} - N\mathcal{H} - N^\rho \mathcal{H}_\rho \right) \right], \tag{27}$$

where the constraint functions are given by

$$\mathcal{H} = \frac{\Lambda P_\Lambda^2}{2R^2} - \frac{P_\Lambda P_R}{R} + \frac{RR''}{\Lambda} - \frac{RR'\Lambda'}{\Lambda^2} + \frac{R'^2}{2\Lambda} - \frac{\Lambda}{2} + \frac{\eta p}{\Lambda} \delta(\rho - r), \tag{28}$$

which is the so-called *super-Hamiltonian*, and

$$\mathcal{H}_\rho = P_R R' - P'_\Lambda \Lambda - p\delta(\rho - r) \quad (29)$$

(the *super-momentum*) and where N, N^ρ are Lagrange multipliers. The variable η takes on two values, -1 for the in- and $+1$ for the outgoing shell and it holds that $\eta = \text{sgn}(p)$. Thus, LWF action is, in fact, a set of two independent actions, each valid for one of the two possible motions. The functions N, N^ρ, R, Λ are to be smooth functions of ρ everywhere, except at the shell, where they are only continuous and may have finite jumps in their first derivatives. Also the conjugate momenta P_R, P_Λ are smooth except at the shell, where they have finite discontinuities. The most singular contributions come from the explicit matter delta-terms in the constraints and the implicit delta-functions appearing in R'' and P'_Λ .

Variation of the action with respect to the canonical variables and the Lagrange multipliers yields the dynamical,

$$\dot{\Lambda} = N \left(\frac{\Lambda P_\Lambda}{R^2} - \frac{P_R}{R} \right) + (N^\rho \Lambda)', \quad (30)$$

$$\dot{R} = -\frac{N P_\Lambda}{R} + N^\rho R', \quad (31)$$

$$\dot{P}_\Lambda = \frac{N}{2} \left[-\frac{P_\Lambda^2}{R^2} - \left(\frac{R'}{\Lambda} \right)^2 + 1 + \frac{2\eta p}{\Lambda^2} \delta(\rho - r) \right] - \frac{N' R R'}{\Lambda^2} + N^\rho P'_\Lambda, \quad (32)$$

$$\dot{P}_R = N \left[\frac{\Lambda P_\Lambda^2}{R^3} - \frac{P_\Lambda P_R}{R^2} - \left(\frac{R'}{\Lambda} \right)' \right] - \left(\frac{N' R}{\Lambda} \right)' + (N^\rho P_R)', \quad (33)$$

$$\dot{r} = \frac{\eta N(r)}{\Lambda(r)} - N^\rho(r), \quad (34)$$

$$\dot{p} = p \left(N^\rho - \frac{\eta N}{\Lambda} \right)'(r), \quad (35)$$

and the constraint equations

$$\mathcal{H} = 0, \quad \mathcal{H}_\rho = 0. \quad (36)$$

The possible occurrence of surface terms has not been taken into account yet, but we will do it after having imposed the fall-off conditions on the metric variables at the infinity $\rho \rightarrow \infty$, that

have been given by Ref. [15] and Kuchař [18]:

$$\Lambda(t, \rho) \approx 1 + \frac{M}{\rho} + O(|\rho|^{-1-\epsilon}), \quad (37)$$

$$R(t, \rho) \approx |\rho| + O(|\rho|^{-\epsilon}), \quad (38)$$

$$P_\Lambda(t, \rho) \approx O(|\rho|^{-\epsilon}), \quad (39)$$

$$P_R(t, \rho) \approx O(|\rho|^{-1-\epsilon}), \quad (40)$$

$$N(t, \rho) \approx N_\infty + O(|\rho|^{-\epsilon}), \quad (41)$$

$$N^\rho(t, \rho) \approx O(|\rho|^{-\epsilon}), \quad (42)$$

where M and N_∞ are functions of t , and where $\epsilon \in (0, 1]$. For a solution, the function $M(t)$ becomes constant and coincides with our parameter M . With these fall-off conditions the asymptotic region ($\rho \rightarrow \infty$) is asymptotically flat. N_∞ is the rate at which the asymptotic Minkowski time T_∞ evolves with respect to the coordinate time t . The variation of the term $\frac{NRR'\Lambda'}{\Lambda^2}$ in the super-Hamiltonian constraint $-N\mathcal{H}$ with respect to Λ leads to the non-vanishing surface term (cf. Ref. [18])

$$N_\infty \lim_{\rho \rightarrow \infty} \left(\frac{RR'}{\Lambda^2} \delta\Lambda \right) = N_\infty \delta M. \quad (43)$$

The surface term (43) can be canceled by adding the so-called ADM boundary term (see also Ref. [19]) to the bulk action:

$$S_\infty = - \int dt (N_\infty E_\infty). \quad (44)$$

4 Removing η and Introducing the Mirror

Our action has to describe both in- and outgoing motions of the shell without this options being predetermined by a chosen value of the variable η . This is easy to arrange by replacing η by $\text{sgn}(p)$. For example, in Eq. (28) η appears in the combination ηp , and we just write $|p|$. The origin of the absolute value here is simply that it is to be the energy of the shell, and the energy E of zero-rest-mass particles and shells is $|p|$ instead of $\sqrt{p^2 + \mu^2}$. The range of p must be extended to $(-\infty, \infty)$ and the sign of p will follow automatically from the equations of motions and the initial and boundary conditions.

At the mirror, the geometry of the solutions is flat similarly as at the infinity and we can choose the boundary conditions on the geometry there by assuming that the foliation at the mirror is special in an analogous way to that at the infinity.

We first suppose that the parameter ρ assumes the fixed value R_m at the mirror,

$$\rho|_m = R_m , \quad (45)$$

and that the foliation is orthogonal to the mirror:

$$N^\rho|_m = 0 . \quad (46)$$

The lapse function can be left arbitrary,

$$N|_m = N_m(t) = \frac{dT}{dt} , \quad (47)$$

where T is the Minkowski time at the mirror. Finally, we require that ρ coincide with R to the first order inclusively:

$$R'|_m = 1 , \quad (48)$$

so that

$$\Lambda|_m = 1 . \quad (49)$$

The modified LWF action reads:

$$S = \int dt \left[p\dot{r} - N_\infty E_\infty + \int_{\rho_m}^\infty d\rho \left(P_\Lambda \dot{\Lambda} + P_R \dot{R} - N\mathcal{H} - N^\rho \mathcal{H}_\rho \right) \right] , \quad (50)$$

where the super-Hamiltonian is:

$$\mathcal{H} = \frac{\Lambda P_\Lambda^2}{2R^2} - \frac{P_\Lambda P_R}{R} + \frac{RR''}{\Lambda} - \frac{RR'\Lambda'}{\Lambda^2} + \frac{R'^2}{2\Lambda} - \frac{\Lambda}{2} + \frac{|p|}{\Lambda} \delta(\rho - r) , \quad (51)$$

The other terms are identical to those in the LWF action. Varying the action (50) with respect to the canonical variables leads to the new *surface term* B_m from the mirror:

$$B_m = \left[\frac{NR}{\Lambda} \delta R' - \frac{NRR'}{\Lambda^2} \delta \Lambda - \frac{N'R}{\Lambda} \delta R + N^\rho P_R \delta R - N^\rho \Lambda \delta P_\Lambda \right]_{\rho=\rho_m} . \quad (52)$$

Inserting Eqs. (45)–(49) into Eq. (52) yields that the boundary term from the mirror vanishes:

$$B_m = 0 .$$

From Eqs. (45)–(49) and Eq. (31), it also follows that the so-called *mass function* Ref. [15],

$$\mathbf{M} = \frac{R}{2} \left[1 - \left(\frac{R'}{\Lambda} \right)^2 + \left(\frac{P_\Lambda}{R} \right)^2 \right]. \quad (53)$$

vanishes at the mirror,

$$\mathbf{M}_m = 0, \quad (54)$$

so that the mass of the mirror is zero as required.

Even with vanishing surface terms B_m , the variation of the action (50) does not lead to the correct equations of motion yet. An additional boundary condition has to be imposed in order that the shell is really reflected at the mirror and does not pass through it unhindered. To incorporate the reflection, the total momentum of the shell at the mirror must be zero:

$$\lim_{t \rightarrow t_m^+} p(t) + \lim_{t \rightarrow t_m^-} p(t) = 0, \quad (55)$$

where t_m is the time of the intersection between the shell and the mirror. This means also that the absolute value of the momentum of the shell does not change, when the shell is reflected by the mirror, and the energy is conserved.

The action (50) with the modified constraint (51), fall-off conditions (37)–(42), the boundary conditions (45)–(49) and (55), as well as the requirements of continuity constitute a complete system determining the evolution so that our space of solutions results. This can be seen as follows.

Outside the mirror, our equations of motion are equivalent to LWF equations except possibly for the explicit requirement that $\text{sgn}(p)$ is constant, which we have not imposed. However, this also follows from the LWF equations of motion. As is shown in Ref. [15], these equations imply that the solution around the shell coincides with Schwarzschild space-time with different mass parameters M_- and M_+ . The difference $M_+ - M_-$ is related to $|p|$ and to the choice of the radial parameter ρ at the shell via Eq. (A2a) of Ref. [15]:

$$|p| = -R(r)\Delta R'(r), \quad (56)$$

Δ meaning the jump across the shell. It follows that $|p|$ cannot vanish, if ρ satisfies the conditions of regularity, i.e., if everywhere $|R'| > \epsilon$, where ϵ is some positive number. As for the sign of p , Eq. (A2b) of Ref. [15] reads

$$p = -\Lambda(r)\Delta P_\Lambda(r). \quad (57)$$

Since p cannot vanish and is equal to a jump of quantities that must evolve continuously to both sides of the shell, it cannot change sign along the shell motion outside the mirror.

At the mirror, however, Eqs. (56) and (57) lose their meaning because there is no inside of the shell to calculate the jump. There, the evolution must be prescribed by hand, and this is done by Eq. (55). It is compatible with $|p|$ changing smoothly and being non-zero, and so it entails that the sign of p must change through the reflection.

5 Reduction

We reduce the action (50) using the same methods as in the case without mirror. The shell's trajectory results from glueing together an in- and an outgoing one at the mirror, in contrast to the system without mirror, where the shell is either in- or outgoing. Thus, in our case, it depends on where the embedding hyper-surface Σ lies, which part of the shell's trajectory it intersects. Σ can even go through the point where the shell hits the mirror. Fig. 3 shows the three possible cases for the embedding hyper-surface.

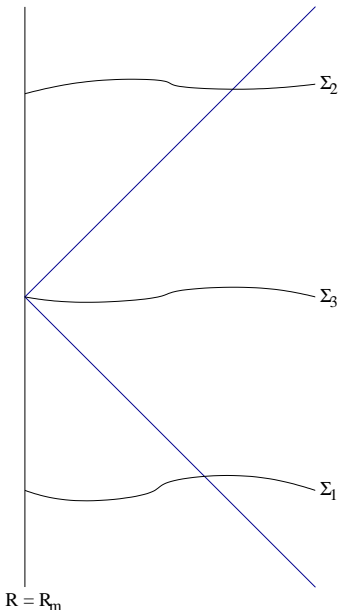


Figure 3: (Color online) Schematic diagram of the trajectory of the shell bouncing at the mirror at the radius $R = R_m$. Three embedding hyper-surfaces Σ are drawn. Σ_1 intersects the in-going shell, Σ_2 the outgoing one. Σ_3 goes through the point where the shell hits the mirror.

For the reduction of the action and for its expression in terms of the Dirac observables, it is not important, which hyper-surface we choose. It will be advantageous to choose a hyper-surface that intersects the outgoing shell, as e.g. Σ_2 in Fig. 3 in the space-time corresponding to the value (M, u) of the Dirac observables. Such a hyper-surface is related to a single point Q , say, at the constraint surface \mathcal{C} in the phase space of the system. All hyper-surfaces in a neighborhood of Σ_2 in the space-time that intersect both the regular center and the outgoing shell determine points in a neighborhood \mathcal{U} of Q at \mathcal{C} . If we carry out this construction for all space-times corresponding to Dirac observables that lie in some neighborhood of the point (M, u) in \mathbf{R}^2 , we fill up a neighborhood \mathcal{U} of Q at \mathcal{C} .

Next, we choose the gauge (U, V) so that we can describe each of the above hypersurfaces by the embedding variables $U(\rho)$ and $V(\rho)$. In this way, we have constructed coordinates $U(\rho)$, $V(\rho)$, M and u in the neighborhood \mathcal{U} in \mathcal{C} (the momenta conjugate to $U(\rho)$ and $V(\rho)$ vanish at \mathcal{C} , see Ref. [5]). We can then, of course, calculate the reduced action in these coordinates. However, we do not need to do this explicitly, for exactly the same calculation has been done, in effect, in Ref. [5]. That is the reason for all the choices above.

In Ref. [5], it is first shown that the reduced action equals to its Liouville form. The Liouville form is expressed in terms of the embedding variables and the shell variables. It is then shown that the Liouville form is determined just by boundary terms at three boundaries: the regular center, the shell and the infinity. The only change to be carried out here is that we have the mirror instead of the regular center. It follows from the expressions in HK that the Liouville form is still given by the boundary terms at the mirror, the shell and the infinity. We have only to find the boundary term resulting from the mirror.

This contribution from the mirror is given by Eq. (60) of Ref. [5] to be

$$-(kdU + ldV)_{\rho=R_m} + \psi|_{\rho=R_m} d\rho_m , \quad (58)$$

where (cf. Eqs. (61) and (62) of Ref. [5])

$$k = \frac{R}{2} \frac{dR}{dU} \ln \left(-\frac{U'}{V'} \right) ,$$

and

$$l = \frac{R}{2} \frac{dR}{dV} \ln \left(-\frac{U'}{V'} \right) .$$

The last term in Eq. (58) vanishes because $\rho_m = R_m$ is constant. Moreover, we have

$$\ln \left(-\frac{U'}{V'} \right) = 0 , \quad (59)$$

because the foliation is orthogonal to the mirror. Indeed, if a radial curve tangential to the mirror is given by $U = U(t)$, $V = V(t)$, $\vartheta = \vartheta_0$ and $\varphi = \varphi_0$, then Eq. (5) implies

$$V(t) - U(t) = 2R_m$$

and the tangent vector $(\dot{U}, \dot{V}, \dot{\vartheta}, \dot{\varphi})$, therefore, satisfies

$$\dot{U} = \dot{V} , \quad \dot{\vartheta} = \dot{\varphi} = 0 . \quad (60)$$

Let the foliation be given by $U = U(t, \rho)$ and $V = V(t, \rho)$. Then, according to Eqs. (1) and (5), the foliation will be orthogonal to the vector fulfilling (60), if

$$-\dot{U}V' - \dot{V}U' = 0$$

or $V' = -U'$, which immediately implies Eq. (59).

It follows that the contribution from the mirror vanishes similarly as that from the regular center did in Ref. [5]. Our Liouville form must, therefore, coincide with that obtained in Ref. [5], and so the reduced action is

$$S = -M\dot{u} . \quad (61)$$

This is equivalent to

$$S = -M\dot{v} . \quad (62)$$

because of Eq. (17). The same results can be obtained if the calculation is carried out along the hyper-surfaces of the type Σ_1 or Σ_3 of Fig. 2, but these have not been described explicitly in Ref. [5].

6 Construction of the shell quantum mechanics

The basic observables we have found in Sec. 5 are the energy E and the asymptotic advanced time v of the shell. They form a canonically conjugate pair: $\{E, v\} = 1$. In this section we turn

these two observables into self-adjoint operators on a suitable Hilbert space. We shall use units for which $c = \hbar = 1$.

For quantization, the ranges of the classical observables are important. While the values of v take the whole real axis, E must be positive and it has been further limited in the classical theory to $E < E_m$ in order that a scattering theory be applicable. We are going to extend this domain to higher energies in quantum theory. However, even in quantum theory, it is impossible that the shell energy is larger than

$$E_o = \frac{R_o}{2G} ,$$

because the shells with $E > E_o$ create a black hole that includes the observer. This is in contradiction with the basic assumption of the scattering theory, namely that the observer is in the asymptotic region, where all interactions are negligible and the geometry of space-time is practically flat. As it will turn out, the scattering theory ceases to be applicable even earlier.

Thus, it is preferable to choose the interval $(0, E_o)$ as the range for E . In this case, unlike to the half axis, a one-dimensional set of self-adjoint operators \hat{v} exists that satisfy the canonical commutation relations with \hat{E} . They are all described in Ref. [20], PP. 141–142.

Let us choose the E -representation so that our Hilbert space can be identified with $L^2(0, E_o)$, the space of square-integrable complex functions $\psi(p)$ on the interval $(0, E_o)$, the action of the operator \hat{E} being

$$\hat{E}\psi(p) = p\psi(p) ; \tag{63}$$

the scalar product is

$$(\psi, \phi) = \int_0^{E_o} dp \psi^*(p) \phi(p) . \tag{64}$$

Then, the self-adjoint operators \hat{v} described in Ref. [20] are defined on the domain \mathcal{D}_θ of the absolutely continuous functions satisfying the boundary conditions

$$\psi(E_o) = e^{i\theta} \psi(0) ,$$

where $\theta \in [0, 2\pi)$, by

$$\hat{v}\psi(p) = -i\partial_p \psi(p) . \tag{65}$$

Clearly, on this domain, the canonical commutation relation are satisfied.

The eigenvalues and eigenfunctions of the thus defined operator \hat{v} are easily shown to be

$$\hat{v}\phi_n(p, \theta) = \frac{2\pi}{E_o}\lambda\phi_n(p, \theta), \quad \lambda = n + \frac{\theta}{2\pi}, \quad n \in \mathbb{Z} \quad (66)$$

and

$$\phi_n(p) = \frac{1}{\sqrt{E_o}}e^{2i\pi\lambda\frac{p}{E_o}}, \quad (\phi_m, \phi_n) = \delta_{mn}. \quad (67)$$

The phase θ appears in the eigenfunctions ϕ_n , so each measurement of the operator \hat{v} will depend on it. We have to choose a particular value of θ . The choice $\theta = 0$ corresponds to the periodical boundary condition often used for the momentum operator in a box. This is surely the simplest choice. With this choice the eigenvalues and -functions of \hat{v} are given by

$$v_n = \frac{2\pi n}{E_o}, \quad n \in \mathbb{Z}, \quad (68)$$

and

$$|v_n\rangle = \phi_n(p) = \frac{1}{\sqrt{E_o}}e^{2i\pi n\frac{p}{E_o}} = \frac{1}{\sqrt{E_o}}e^{iv_n p}. \quad (69)$$

The spectrum of \hat{v} is discrete. This is the price we have to pay for making the operator self-adjoint on a finite interval. The discreteness of the spectrum does not seem to correspond to a realistic physical situation, where the asymptotic advanced time takes values from a continuous spectrum. But the situation is not so bad as it seems if we look at the distance between two neighboring eigenvalues, $d = v_{n+1} - v_n$: The distance

$$d = \frac{2\pi}{E_o} = \frac{2\pi\hbar c}{E_o} \quad (70)$$

becomes very small, $d \ll 1$, so that the spectrum can be considered 'almost continuous'. Indeed, $E_o \approx 100 M_{\text{Earth}}$ for $R_o \approx 1 m$, and $d \approx 10^{-66} m$.

The eigenstates of \hat{v} define the Fourier transform from v - to p -representation

$$\psi(p) = \frac{1}{\sqrt{E_o}} \sum_{n=-\infty}^{\infty} e^{2i\pi n\frac{p}{E_o}} \tilde{\psi}(n) \quad (71)$$

and its inverse,

$$\tilde{\psi}(n) = \frac{1}{\sqrt{E_o}} \int_0^{E_o} dp e^{-2i\pi n\frac{p}{E_o}} \psi(p). \quad (72)$$

The final step in constructing a quantum theory is a choice of dynamics. In our case, there is a time-translation symmetry given by Eqs. (21); the corresponding change of Dirac observables

described by Eqs. (22) is canonically generated by the energy E . Hence, the most natural choice of Hamiltonian is $\hat{H} = \hat{E}$ (see Ref. [7]).

Let us work in Schrödinger picture so that the wave function acquires the time dependence

$$\psi(p)e^{-ipt} .$$

This, of course, makes expected values of \hat{v} time dependent. The interpretation of this time dependence is, as explained in Ref. [7], that a time-shifted observer will see a different value of v in the same state. For example,

$$\int_0^{E_o} dp \psi_n^*(p) e^{ipt} \hat{v} [\psi_n(p) e^{-ipt}] = v_n - t ,$$

which is in agreement with Eqs. (22) for $\tau = -t$, that is, for an observer shifted by the amount $+t$ of time. There is no contradiction in the claim that the expected value of \hat{v} in a state is not equal to some eigenvalue of \hat{v} .

7 The scattering times

In this section, we construct operators from the classical observables $s_{\pm}(R_o)$ and $s(R_o)$ for the whole range of the energy $E \in (0, E_o)$ and show that their expected values and spreads are finite in reasonable states.

We define in p -representation:

$$\hat{s}_-(R_o) = -i \frac{\partial}{\partial p} - R_o \quad (73)$$

and

$$\hat{s}(R_o) = \sqrt{1 - \frac{2Gp}{R_o}} \left[2(R_o - R_m) + 4Gp \ln \left| \frac{1 - \frac{2Gp}{R_o}}{\frac{R_m}{R_o} - \frac{2Gp}{R_o}} \right| \right] . \quad (74)$$

The multiplicative operator $\hat{s}(R_o)$ is indeed well-defined on all continuous functions $\psi(p)$ because the result of its action on such functions is square integrable.

Observe also that we can write Eq. (74) in a scale-invariant form

$$\frac{\hat{s}(R_o)}{R_o} = 2\sqrt{1 - q} \left(1 - \rho + q \ln \left| \frac{1 - q}{\rho - q} \right| \right) , \quad (75)$$

where

$$\rho = \frac{R_m}{R_o} < 1$$

and

$$q = \frac{p}{E_o} \leq 1$$

are dimension-free quantities. The existence of such a formula is related to the dilatation symmetry of the classical theory. On the other hand, Eq. (73) cannot be written in such a form and we have only

$$\frac{\hat{s}_-(R_o)}{R_o} = -i \frac{2G}{R_o^2} \frac{\partial}{\partial q} - 1 ,$$

because the canonical commutation rules break the dilatation symmetry.

7.1 Eigenstates of \hat{v}

The calculation of $\langle v_n | \hat{s}(R_o) | v_n \rangle$ or $\langle v_n | [\hat{s}(R_o)]^2 | v_n \rangle$ is straightforward but tedious. All other expected values and spreads are, however, easily expressible in terms of these two. For example, we have

$$\begin{aligned} & \langle v_n | [\hat{s}_-(R_o) + \hat{s}(R_o)]^2 | v_n \rangle \\ &= \langle v_n | [\hat{s}_-(R_o)]^2 | v_n \rangle + \langle v_n | [\hat{s}(R_o)]^2 | v_n \rangle + 2 \left| \sum_m \langle v_n | \hat{s}(R_o) | v_m \rangle \langle v_m | \hat{s}_-(R_o) | v_n \rangle \right| \\ &= \langle v_n | [\hat{s}_-(R_o)]^2 | v_n \rangle + \langle v_n | [\hat{s}(R_o)]^2 | v_n \rangle + 2 \langle v_n | \hat{s}(R_o) | v_n \rangle \langle v_n | \hat{s}_-(R_o) | v_n \rangle \end{aligned} \quad (76)$$

because the operator $\hat{s}_-(R_o)$ is diagonal in the basis $|v_n\rangle$.

Our method of calculation will be based on the formula

$$\int dq X(q) \ln |q - \xi| = [Y(q) - Y(\xi)] \ln |q - \xi| - \int dq \frac{Y(q) - Y(\xi)}{q - \xi} , \quad (77)$$

where $Y(q)$ is any primitive function to $X(q)$,

$$Y(q) = \int dq X(q) .$$

(The integration per partes is just performed here with the choice of the primitive function that makes the resulting formula manifestly regular.)

Using Eqs. (69) and (75), we obtain

$$\begin{aligned} \frac{1}{R_o} \langle v_n | \hat{s}(R_o) | v_n \rangle &= 2 \int_0^1 dq \sqrt{1-q} (1 - \rho + q \ln |q - 1| - q \ln |q - \rho|) \\ &= -\frac{4}{3} (1 - \rho) (1 - q)^{3/2} \Big|_0^1 + 2 \int_0^1 dq q \sqrt{1-q} \ln |q - 1| - 2 \int_0^1 dq q \sqrt{1-q} \ln |q - \rho| . \end{aligned} \quad (78)$$

Now,

$$\int dq q \sqrt{1-q} = -\frac{2}{15}(2+q-3q^2)\sqrt{1-q},$$

and we obtain from formula (77), first,

$$\begin{aligned} & \int_0^1 dq q \sqrt{1-q} \ln |q-1| \\ &= -\frac{2}{15}(2+q-3q^2)\sqrt{1-q} \ln |q-1| \Big|_0^1 + \frac{2}{15} \int_0^1 dq \frac{(2+q-3q^2)\sqrt{1-q}}{q-1} \\ &= -\frac{2}{15} \int_0^1 dq \sqrt{1-q}(2+3q) = -\left(\frac{8}{15}\right)^2 \end{aligned}$$

and, second,

$$\begin{aligned} & \int_0^1 dq q \sqrt{1-q} \ln |q-\rho| \\ &= -\frac{2}{15} \left[(2+q-3q^2)\sqrt{1-q} - (2+\rho-3\rho^2)\sqrt{1-\rho} \right] \ln |q-\rho| \Big|_0^1 \\ & \quad + \frac{2}{15} \int_0^1 dq \frac{(2+q-3q^2)\sqrt{1-q} - (2+\rho-3\rho^2)\sqrt{1-\rho}}{q-\rho} \\ &= -\frac{4 \times 31}{15^2} - \frac{8}{15}\rho + \frac{2}{15} [2 - (2+\rho-3\rho^2)\sqrt{1-\rho}] \ln \rho + \frac{4}{15} (2+\rho-3\rho^2)\sqrt{1-\rho} \ln(1+\sqrt{1-\rho}). \end{aligned}$$

In order to see, what this complicated formula means, we expand it in powers of ρ and $\ln \rho$, neglecting all terms with ρ^2 , $\rho^2 \ln \rho$ and higher. The result is independent of ρ !

$$\frac{1}{R_o} \langle v_n | \hat{s}(R_o) | v_n \rangle = \frac{4}{15} (7 - 4 \ln 2). \quad (79)$$

Observe that the corresponding classical result for the flat space-time is $2(1-\rho)$ and so the quantum scattering time is shorter than the classical flat space-time one if $\rho < (1+8 \ln 2)/15$, which is surely the case for all $\rho \ll 1$. This is due to the broad spread of energy in the state $|v_n\rangle$ and the factor $\sqrt{1-q}$ in the integral because q runs up to 1 in the quantum theory: the massive shells “shorten” the proper time interval measured by the external observer. The independence of the formula on v_n is clearly due to the time-translation invariance of the model.

The expected value of the square of the scattering time operator in the state $|v_n\rangle$ is given by

$$\begin{aligned} \frac{1}{R_o^2} \langle v_n | (\hat{s}(R_o))^2 | v_n \rangle &= \frac{4}{3} - \frac{5}{3}\rho - \frac{2}{3}\rho^2 + \rho^3 + \left(\frac{2}{3} - \frac{11}{3}\rho + 2\rho^2 + \rho^3 \right) \rho \ln \rho \\ & \quad + (-1 + 2\rho^2 - \rho^4) \ln(1-\rho) + \left(\frac{4}{3} - \rho \right) \rho^3 \ln^2 \rho + \frac{2}{3} (1 - 4\rho^3 + 3\rho^4) \left(\frac{\pi^2}{3} - \text{dilog } \rho \right) \quad (80) \end{aligned}$$

where the dilogarithmic function is defined by

$$\text{dilog } x := \int dx \frac{\ln x}{1-x}.$$

Expansion in ρ yields that also the squared scattering time operator does not depend on ρ up to first order:

$$\frac{1}{R_o^2} \langle v_n | (\hat{s}(R_o))^2 | v_n \rangle \approx \frac{4}{3} + \frac{1}{9} \pi^2. \quad (81)$$

Here we have used the expansion of the dilogarithm,

$$\text{dilog } \rho \approx \frac{\pi^2}{6} - \rho + \rho \ln \rho + \mathcal{O}(\rho^2, \rho^2 \ln \rho).$$

The mean value of the operator $\hat{s}_-(R_o)$ is simply obtained:

$$\langle v_n | \hat{s}_-(R_o) | v_n \rangle = -R_o + \frac{2\pi n}{E_o}. \quad (82)$$

That of its square reads

$$\langle v_n | \hat{s}_-^2(R_o) | v_n \rangle = R_o^2 - \frac{4\pi n R_o}{E_o} + \frac{4\pi^2 n^2}{E_o^2}, \quad (83)$$

thus the spread vanishes, as expected:

$$(\Delta s_-)_n = 0. \quad (84)$$

The expected value of the operator \hat{s}_+ is easily found by using the formulae (78) and (82). Its square can be obtained by using Eqs. (76), (80), (82) and (83). Expanding in ρ as above, one finds the spread of \hat{s}_+ to be independent on ρ and on the state $|v_n\rangle$:

$$\frac{\Delta s_+(R_o)}{R_o} \approx \sqrt{\frac{4}{3} + \frac{\pi^2}{9} - \frac{4}{15}(7 - 4 \ln 2)} \approx 1.1413. \quad (85)$$

We observe that everything has a well-defined limit as $\rho \rightarrow 0$.

7.2 Energy dependence of the scattering time

In this subsection, we are going to study the behavior of the scattering times with energy. To that aim, we have to work with suitable wave packets $\phi(p)$. For example, to calculate $\langle \phi | \hat{s}(R_o) | \phi \rangle$ and $\langle \phi | [\hat{s}(R_o)]^2 | \phi \rangle$, one can take the so-called box wave packets,

$$\phi(p) = 0 \quad \forall p \in (0, E_o(\bar{q} - w/2)) \cup (E_o(\bar{q} + w/2), E_o)$$

and

$$\phi(p) = \frac{1}{\sqrt{E_o w}} \quad \forall p \in (E_o[\bar{q} - w/2], E_o[\bar{q} + w/2]) ,$$

where $E_o\bar{q}$ is the mean energy and $E_o w$ the width of the packet, \bar{q} and w being the corresponding dimension-free quantities. Operators containing \hat{v} or \hat{v}^2 may then have diverging expected values. However, the box wave packets are completely sufficient and perfectly suitable for the study of the energy dependence of the scattering time and its spread.

Analogously to the preceding subsection the expected values can be written in terms of the dimension-free quantities:

$$\frac{1}{R_o} \langle \phi | \hat{s}(R_o) | \phi \rangle = \frac{1}{w} \int_{\bar{q}-w/2}^{\bar{q}+w/2} dq F(\rho, q) \quad (86)$$

and

$$\frac{1}{R_o^2} \langle \phi | [\hat{s}(R_o)]^2 | \phi \rangle = \frac{1}{w} \int_{\bar{q}-w/2}^{\bar{q}+w/2} dq F^2(\rho, q) , \quad (87)$$

where we have used the abbreviation

$$F(\rho, q) := 2\sqrt{1-q} \left(1 - \rho + q \ln \left| \frac{1-q}{\rho-q} \right| \right) .$$

The spread is

$$\frac{\Delta \hat{s}(R_o)}{R_o} = \sqrt{\frac{1}{R_o^2} \langle \phi | [\hat{s}(R_o)]^2 | \phi \rangle - \frac{1}{R_o^2} [\langle \phi | \hat{s}(R_o) | \phi \rangle]^2} . \quad (88)$$

The integrands are the same as in the case of the v -eigenstates and the integrals can be computed in a completely analogous manner. Since they are rather unwieldy, we will not write down the results explicitly but rather derive important properties of the expected values using suitable approximations.

In the interval

$$0 < q \ll \rho ,$$

we can expand F in powers of q :

$$F(\rho, q) \approx 2(1 - \rho) - (2 \ln \rho + 1 - \rho)q + \dots .$$

Integrating term by term, we obtain

$$\frac{1}{R_o} \langle \phi | \hat{s}(R_o) | \phi \rangle \approx 2(1 - \rho) - (2 \ln \rho + 1 - \rho)\bar{q} ,$$

and the leading term is the flat space-time value as expected. Numerical study of the function F shows that the expected value (86) is increasing in the whole interval $0 < \bar{q} < \rho$.

At $\bar{q} = \rho$, the integral in Eq. (86) can be written as follows

$$\frac{1}{w} \int_{\rho-w/2}^{\rho+w/2} dq F(\rho, q) = \frac{1}{w} \int_{\rho-w/2}^{\rho+w/2} dq a(q) - \frac{1}{w} \int_{\rho-w/2}^{\rho+w/2} dq b(q) \ln |q - \rho| ,$$

where

$$a(q) := 2\sqrt{1-q} [1 - \rho + q \ln(1 - q)]$$

and

$$b(q) := 2q\sqrt{1-q}$$

are smooth functions in a neighborhood of $q = \rho$. We are going to expand the integrals in powers of w and of $\ln(w/2)$. We observe first that

$$\frac{1}{w} \int_{\rho-w/2}^{\rho+w/2} dq a(q) = a(\rho) + O(w) \quad (89)$$

for any C^1 function $a(q)$. Second, we can use the trick of the foregoing subsection:

$$\begin{aligned} \frac{1}{w} \int_{\rho-w/2}^{\rho+w/2} dq b(q) \ln |q - \rho| \\ = \frac{1}{w} \{ [b_1(q) - b_1(\rho)] \ln |q - \rho| \}_{\rho-w/2}^{\rho+w/2} - \frac{1}{w} \int_{\rho-w/2}^{\rho+w/2} dq \frac{b_1(q) - b_1(\rho)}{q - \rho} , \end{aligned}$$

where $b'_1(q) = b(q)$ so that

$$\lim_{q \rightarrow \rho} \frac{b_1(q) - b_1(\rho)}{q - \rho} = b(\rho) .$$

Hence, if $b(q)$ is any smooth function,

$$\frac{1}{w} \int_{\rho-w/2}^{\rho+w/2} dq b(q) \ln |q - \rho| = -b(\rho) + b(\rho) \ln(w/2) + O[w \ln(w/2)] . \quad (90)$$

Collecting all results, we obtain

$$\frac{1}{R_o} \langle \phi | \hat{s}(R_o) | \phi \rangle = 2\sqrt{1-\rho} [1 + \rho \ln(1 - \rho) - \rho \ln(w/2)] + O[w \ln(w/2)] . \quad (91)$$

There is a sharp peak at $\bar{q} = \rho$ that grows like $-\ln \frac{w}{2}$. From this we infer that the scattering time displays a kind of *resonance* phenomenon near the critical energy, $\bar{q} \approx \rho$. The resonance gets more distinct when the packet becomes narrower.

The integral in Eq. (87) can be dealt with in an analogous way. First,

$$\begin{aligned} \frac{1}{w} \int_{\rho-w/2}^{\rho+w/2} dq F^2(\rho, q) &= \frac{1}{w} \int_{\rho-w/2}^{\rho+w/2} dq \bar{a}(q) \\ &\quad - \frac{1}{w} \int_{\rho-w/2}^{\rho+w/2} dq \bar{b}(q) \ln |q - \rho| + \frac{1}{w} \int_{\rho-w/2}^{\rho+w/2} dq \bar{c}(q) \ln^2 |q - \rho| , \end{aligned}$$

where

$$\begin{aligned} \bar{a}(q) &:= 4(1-q)[1-\rho+q\ln(1-q)]^2 , \\ \bar{b}(q) &:= 8(1-q)q[1-\rho+q\ln(1-q)] \end{aligned}$$

and

$$\bar{c}(q) := 4(1-q)q^2$$

are smooth functions in a neighborhood of $q = \rho$. Thus, for the first two integrals, we can use the formulae (89) and (90). The third integral can be written as follows

$$\begin{aligned} \frac{1}{w} \int_{\rho-w/2}^{\rho+w/2} dq \bar{c}(q) \ln^2 |q - \rho| &= \frac{1}{w} \{ [\bar{c}_1(q) - \bar{c}_1(\rho)] \ln^2 |q - \rho| \}_{\rho-w/2}^{\rho+w/2} \\ &\quad - \frac{1}{w} \int_{\rho-w/2}^{\rho+w/2} dq 2 \frac{\bar{c}_1(q) - \bar{c}_1(\rho)}{q - \rho} \ln |q - \rho| , \end{aligned}$$

where $\bar{c}'_1(q) = \bar{c}(q)$ and the function

$$\bar{c}_2(q) := 2 \frac{\bar{c}_1(q) - \bar{c}_1(\rho)}{q - \rho}$$

is smooth in a neighborhood of $q = \rho$ with $\bar{c}_2(\rho) = \bar{c}(\rho)$. Again, we use Eq. (90) and obtain

$$\begin{aligned} \frac{1}{R_o^2} \langle \phi | (\hat{s}(R_o))^2 | \phi \rangle &= 4(1-\rho)\rho [\rho - 4\ln(1-\rho)] \\ &\quad + 4(1-\rho)[1 + \rho\ln(1-\rho) - \rho\ln(w/2)]^2 + O(w\ln^2(w/2)) . \end{aligned} \quad (92)$$

It follows that the spread of the scattering time at $\bar{q} = \rho$ attains a regular limit for $w \rightarrow 0$ and in this sense is relatively weakly dependent on w :

$$\frac{\Delta \hat{s}(R_o)}{R_o} = 2\sqrt{(1-\rho)\rho [\rho - 4\ln(1-\rho)]} + O(w\ln^2(w/2)) . \quad (93)$$

Finally, in the interval

$$\rho < q < 1 ,$$

numerical analysis shows that F first steeply falls to a minimum, then slowly increases reaching its second maximum if ρ is smaller than about 0.1, and then falls again to negative values near $q = 1$. Near its local maximum, F is of course slowly changing and the scattering time is in a very good approximation equal to the value of F there (for small w). Expanding F and $\partial F/\partial q$ in powers of ρ , we find that the position and the value of the second maximum depends only weakly on ρ ; the corrections to results obtained for $\rho = 0$ are of the second order in ρ . Thus, we obtain for the position $q_M(\rho)$ of the second maximum

$$q_M(\rho) = q_M(0) + O(\rho^2) ,$$

where $q_M(0)$ is the larger solution to the equation $\partial F/\partial q(0, q) = 0$, which reads

$$\ln \frac{1-q}{q} = \frac{3}{2-3q} ,$$

and the value $F_M(\rho)$ of the second maximum is

$$\frac{F_M(\rho)}{R_o} = \frac{F_M(0)}{R_o} + O(\rho^2) ,$$

where $F_M(0)$ is the value of the second maximum of $F(0, q)$, or

$$\frac{F_M(0)}{R_o} = \frac{4\sqrt{1-q_M(0)}}{2-3q_M(0)} .$$

Numerical calculations yield

$$q_M(0) = .133071$$

and

$$\frac{F_M(0)}{R_o} = 2.32658 .$$

We observe first that the second maximum lies at very high energies. If an observer is going to send a shell from the radius, say, 1 m to the center, then the energy needed to achieve the scattering time corresponding to the second maximum lies at about 25 Earth masses. The existence of the second maximum and the fall in the scattering time at still higher energies result from the manipulations of the observer proper time and of his position in the space-time due to this huge mass concentration rather than from some processes near and under the horizon. The second observation is that the value of the second maximum is not much larger than $2R_o$, which corresponds roughly to the flat space-time value. The plot of the resonance behavior of the time (86) for some typical values of ρ and w in a reasonable energy interval is given in Fig. 4.

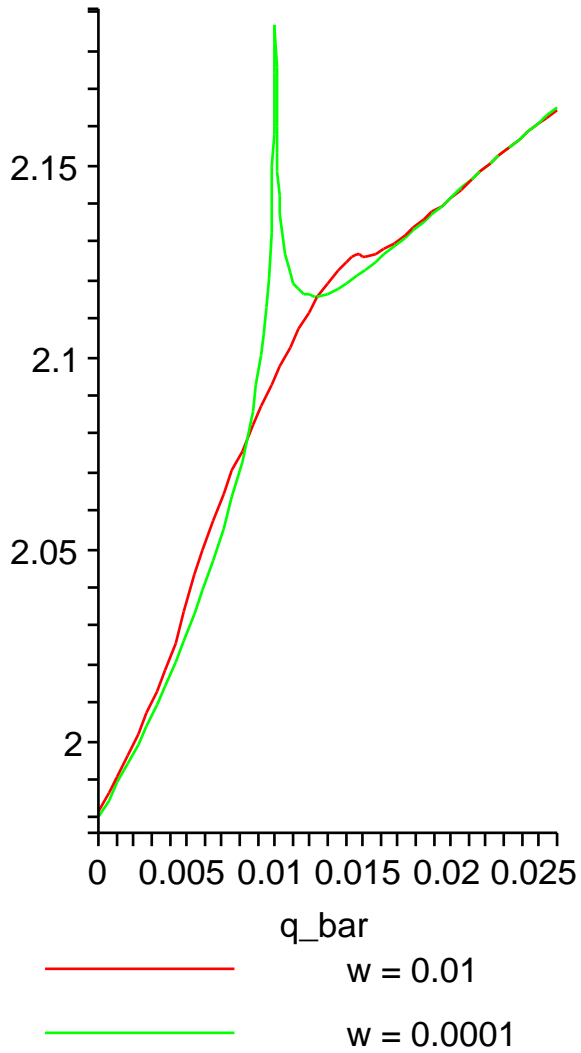


Figure 4: (Color online) The expected scattering time $\frac{1}{R_o} \langle \phi | \hat{s}(R_o) | \phi \rangle$ for box wave packets is plotted as a function of the dimension-free mean energy \bar{q} . Plots are shown for packets with constant energy widths $w = 0.01$ and $w = 0.0001$. The mean scattering time has a peak near the critical energy at $\rho = 0.01$. The peak is more distinctive when the packet is narrower.

8 Discussion

The values of the scattering times calculated in the previous section are roughly comparable to the time $2(R_o - R_m)$ the light needs to cross twice the flat space-time distance between the observer and the mirror. It can be appreciably shorter if the wave packet contains sufficiently strong high-energy part ($\bar{q} \approx 1$), or much larger, if it is concentrated at the resonant energy ($\bar{q} \approx \rho$). Although the resonance can yield arbitrarily long scattering times, it works only in an extremely narrow regime of \bar{q} and w . Hence, our quantum theory does not yield black-hole-like objects with their observed properties.

Quite a number of excuses can be thought of. One class of explanations might be based on the obvious difference between our shell model and a real astrophysical object. For example, the collapse of the shell is a one-off event while an astrophysical black hole must be fed steadily in order to be observable; the zero-rest-mass shell is rather different from a massive star; etc. Another class contains explanations that seek the reason for too short scattering times in our calculation method. Could the model of thin null shell be kept and only the ideas changed of how the scattering time is defined and calculated? Let us focus on this second possibility.

Some freedom of this class is the usual ambiguity in factor orderings and in the choice of self-adjoint extensions, such as, in our case, the freedom in the parameter θ in Eq. (66). It seems, however, that different choices of this kind are rather unlikely to change the scattering times a great deal. Some hopeful freedom seems to be the following.

Our quantum calculation is based on the classical formula (23) that has been changed in two ways. First, it is extended for energies in the interval $(0, E_m)$ to the interval $(0, E_o)$ by replacing the parenthesis under the logarithm by the absolute value signs:

$$s(R_o) = \sqrt{1 - \frac{2GE}{R_o}} \left[2(R_o - R_m) + 4GE \ln \left| \frac{R_o - 2GE}{R_m - 2GE} \right| \right]. \quad (94)$$

Second, this extended formula is turned into an operator. Can the formula (94) be given any “classical” meaning for $E > E_m$?

To see how this might be possible, consider first classical shells with energies smaller than E_m . Then the space-time outside the shell can be foliated by space-like surfaces of constant Schwarzschild time T . Let us denote by T_m the Schwarzschild time of the encounter between

the shell and the mirror, and by T_{\pm} those between the shell and the observer. One easily verifies that

$$s(R_o) = \sqrt{1 - \frac{2GE}{R_o}} [2(T_- - T_m)] . \quad (95)$$

Next, this formula can be extended to higher energies as follows. Consider an in-going shell solution with $E > E_m$. Even then, the Schwarzschild time coordinate T is well-defined everywhere outside the shell (up to a constant shift, which has no influence on the results). The differences to the $E < E_m$ case are that there is the *internal* Schwarzschild time for the part of the space-time that lies inside the horizon, and the *external* Schwarzschild time outside; that the levels of the internal time are time-like; and that each of these “times” runs itself through the whole real axis (in the maximal—Kruskal—extension of Schwarzschild space-time). Therefore, the value T_- (of the external) and T_m (of the internal time) are both well defined in this case, too, and one can again easily verify that Eq. (95) gives the same answer as Eq. (94).

The formula (95) has an interpretation in terms of space-times and foliations even for $E > E_m$. Indeed, the external Schwarzschild time coordinate runs through all real values along the in-going shell, starting by $-\infty$ at \mathcal{I}^- and reaching $+\infty$ at the horizon, $R = 2GE$. Hence, the external Schwarzschild time takes on the value T_m somewhere at the shell trajectory outside the horizon; let us denote the radius of this point by R'_m ; clearly, $R'_m > 2GE > R_m$. Hence, there is a surface, Σ' , consisting of two pieces: the first is the shell trajectory from the radius R_m to the radius R'_m and the second is the part of the surface $T = T_m$ from R'_m to $R = \infty$. Σ' is a non-time-like surface; it can, therefore, be slightly deformed to a smooth spherically symmetric *space-like* surface Σ'' that runs from the intersection of the in-going shell with the mirror at $R = R_m$ inside the horizon until it meets the $T = T_m$ surface outside the horizon at $R = R'_m + \epsilon$, where ϵ is any given real number larger than zero that can be arbitrarily small. Afterwards, Σ'' coincides with the surface $T = T_m$ for $R \in (R_m + \epsilon, \infty)$. The construction is displayed in Fig. 5.

Suppose that $R'_m < R_o$ so that the scattering time will be positive. Then the construction of a “classical” space-time with a reflected shell and the scattering time given by Eq. (95) is as follows. Let us cut the in-going-shell space-time along Σ'' , throw away the future part and denote the remaining space-time by \mathcal{M}''_- . Let us further define another piece \mathcal{M}''_+ of space-time as the time-reversal of \mathcal{M}''_- that is given by Eq. (10) with an arbitrary choice of parameter u . Finally paste together \mathcal{M}''_- with \mathcal{M}''_+ along Σ'' and its time reversal Σ''_+ in \mathcal{M}''_+ so that

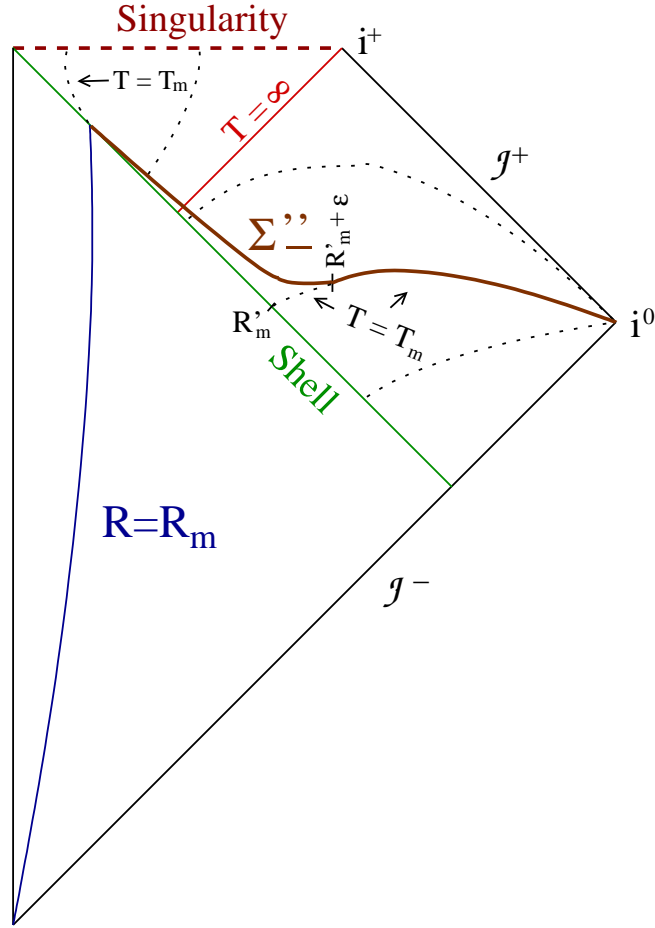


Figure 5: (Color online) The construction of the 3-surface Σ'' . The dotted lines are the 3-surfaces of constant external and internal Schwarzschild time. The space-time above the shell is Schwarzschild and below it is Minkowski one. The observer trajectory is not shown, but if it crossed the shell at $T_- > T_m$, the scattering time would be negative.

spheres of the same radius coincide. The resulting space-time \mathcal{M}'' has a continuous metric which is piecewise smooth, but only C^0 at Σ'' between the radii R_m and $R'_m + \epsilon$ and at the shell; observe that it is smooth at Σ'' for $R > R'_m + \epsilon$ because of the time-reversal properties of Schwarzschild space-times mentioned in the Introduction. The shell is reflected at the mirror that forms a boundary of \mathcal{M}'' and the corresponding scattering time is again given by Eq. (94) for any $E \in (0, E_o)$.

The use of the time reversal in the construction is not accidental. Each space-time with the outgoing shell that has the same energy and with the mirror that has the same radius as our in-going-shell space-time is a time reversal (10) of the in-going-shell space-time. Hence, the space-time that describes the reflection of the shell at the mirror can also be constructed by pasting these in-going- and outgoing-shell space-times along some space-like 3-surfaces that cross the mirror at the shell-reflection points. One of these surfaces lies in the in-going-, the other in the outgoing-shell space-time. The surfaces must be isometric to each other or else they will not match each other and the resulting metric will not be C^0 at the pasting points. One can then easily verify that the two 3-surfaces must also be related by the time reversal.

Let us call “fold” any space-like 3-surface where the metric is only C^0 . Of course, the folds do not make much sense from the classical general relativity point of view. A space-time with folds can, however, be used as a possible path in the calculation of a path integral defined by the Feynman-Kac formula (Ref. [20], Sec. X.11). Similar space-times have been described in Refs. [21] and [6]. Observe that the folds in any polygonal “zig-zag” path lie at the surfaces of constant time and their form is, therefore, influenced by the chosen foliation. The scattering time depends not only on the number of folds, but also on the foliation, as mentioned in the Introduction.

Even if one would take this polygonal space-time idea seriously, one could see at once that it opens new freedom in addition to giving an interpretation of Eq. (94). Why the internal Schwarzschild time T_m of the reflection is to coincide with the external Schwarzschild time T'' at which the two space-time pieces \mathcal{M}''_- and \mathcal{M}''_+ are to be pasted together for the radii $R > R''$ ($R'' = R'_m + \epsilon$ in the above construction)? Clearly, similar constructions can be carried out for *any* value of T'' whatsoever because the external Schwarzschild time runs through all real values along the shell. This shows explicitly how different foliations can lead to very different

scattering times.

In fact, it seems that the foliation ought to be chosen such that the folds are limited to a region with as small radius as possible. Recall that the constructed space-time had a regular (smooth) classical metric outside R'' . Sure, for $E > E_m$, there is no classical solution interpolating between the two asymptotic (in- and outgoing) states of the shell that does not pass at least through one fold, but the folds could be banished to the inside of the horizon in this way. Thus, the resulting quantum geometry could be very similar to the classical Schwarzschild geometry outside the horizon, while it had to differ strongly from it inside. At the same time, the condition that the folds must not protrude too much through the horizon would also lead to long scattering times (they have to go out of the horizon at least a little because they have to meet the 3-surfaces of constant external Schwarzschild time). This follows from the fact that $T'' \rightarrow \infty$ along the shell as R'' approaches the horizon.

One possible conclusion from this discussion is that the quantum theory of gravitational collapse does not entail any natural formula for the scattering time. More precisely, the differences in scattering times of one and the same scattering process arising from various possible definitions of scattering time cannot be attributed only to different choices of factor orderings (because their order of magnitude is much larger than that of the Planck constant). This seems to leave some hope that a method (or even a new principle) exists, which 1) can be better justified than Eq. (94) and 2) would lead to considerably longer scattering times. More research is needed, before a clear understanding can be established.

References

- [1] S. W. Hawking, G. F. R. Ellis, *The Large Scale Structure of Space-Time*, Cambridge University Press, Cambridge, 1973.
- [2] S. W. Hawking, *Commun. Math. Phys.* **87**, 395 (1982); T. Banks, M. E. Peskin and L. Susskind, *Nucl. Phys.* **B244**, 125 (1984).
- [3] A. D. Sacharov, *JETP* **22**, 241 (1966).
- [4] S. A. Hayward, arXiv: gr-qc/0506126.

- [5] P. Hájíček and C. Kiefer, Nucl. Phys. **B 603**, 491 (2001).
- [6] P. Hájíček, Nucl. Phys. **B 603**, 515 (2001).
- [7] P. Hájíček, in *Quantum Gravity. From Theory to Experimental Search*, Eds. D. Giulini, C. Kiefer and C. Lämmerzahl, Springer, Berlin, 2003. ArXive: gr-qc/0204049.
- [8] P. Hájíček, Nucl. Phys. B (Proc. Suppl.) **80** (2000) CD-ROM supplement. ArXive: gr-qc/9903089.
- [9] M. L. Goldberger and K. M. Watson, *Collision theory*, Wiley, New York, 1964.
- [10] P. A. Martin, Acta Phys. Aust. Suppl. **23**, 157 (1981).
- [11] J. D. Dollard, J. Math. Phys. **5**, 729 (1964).
- [12] D. Bollé, F. Gesztesy and H. Grosse, J. Math. Phys. **24**, 1529 (1983).
- [13] K. V. Kuchař, in G. Kunstatter et al. (Eds.), *Proceedings of the 4th Canadian Conference on General Relativity and Relativistic Astrophysics*, World Scientific, Singapore, 1992.
- [14] C. J. Isham, in *Integrable Systems, Quantum Groups and Quantum Field Theories*, Kluwer Academic Publishers, London, 1993.
- [15] J. Louko, B. Whiting and J. Friedman, Phys. Rev. D **57**, 2279 (1998).
- [16] P. Hájíček and I. Kouletsis, Class. Quantum Grav. **19**, 2529 (2002); *ibid.* **19**, 2551 (2002); I. Kouletsis and P. Hájíček, *ibid.* **19**, 2567 (2002).
- [17] M. Ambrus, *How long does it take until a quantum system reemerges after a gravitational collapse?*, Inauguraldissertation, University of Berne, 2004.
- [18] K. V. Kuchař, Phys. Rev. **D50**, 3961 (1994).
- [19] T. Regge and C. Teitelboim, Ann. Phys. **88**, 286 (1974).
- [20] M. Reed and B. Simon, *Methods of modern mathematical physics II. Fourier analysis, self-adjointness*, Acad. Press, New York, 1975.
- [21] C. R. Stephens, G.'t Hooft, and B. F. Whiting, Class. Quantum Grav. **11**, 621 (1994).